Flux Pileup in Collisionless Magnetic Reconnection: Bursty Interaction of Large Flux Ropes

H. Karimabadi,[1] J. Dorelli,[2] V. Roytershteyn,[1] W. Daughton,[3] and L. Chacón[4]
[1]University of California at San Diego, La Jolla, California 92093, USA
[2]NASA Goddard Space Flight Center, Maryland 20771, USA
[3]Los Alamos National Laboratory, Los Alamos, New Mexico 87544, USA
[4]Oak Ridge National Laboratory, Oak Ridge, Tennessee 37830, USA
(Received 10 March 2011; published 6 July 2011)

Using fully kinetic simulations of the island coalescence problem for a range of system sizes greatly exceeding kinetic scales, the phenomenon of flux pileup in the collisionless regime is demonstrated. While small islands on the scale of $\lambda \leq 5$ ion inertial length (d_i) coalesce rapidly and do not support significant flux pileup, coalescence of larger islands is characterized by large flux pileup and a weaker time averaged reconnection rate that scales as $\sqrt{d_i/\lambda}$ while the peak rate remains nearly independent of island size. For the largest islands ($\lambda = 100 d_i$), reconnection is bursty and nearly shuts off after the first bounce, reconnecting ~20% of the available flux.

DOI: 10.1103/PhysRevLett.107.025002 PACS numbers: 52.35.Vd, 94.30.cp, 96.50.Pw, 96.60.Iv

Magnetic reconnection is often invoked to explain the rapid, often impulsive, conversion of magnetic energy into plasma energy in both astrophysical and laboratory plasmas. Many of these environments are characterized by system size much larger than kinetic scales and near or fully collisionless conditions. One important type of problem involving reconnection is the formation and subsequent interaction of flux ropes as observed in planetary magnetospheres, the solar wind, and in the solar corona. A simple configuration to model the flux rope interaction is the pairwise coalescence of magnetic islands [1].

The coalescence process is driven by the attraction of currents associated with two neighboring islands [1]. As the islands approach each other, a current sheet is formed between them which can become susceptible to reconnection. In the absence of reconnection, the magnetic field between the two islands would pileup until the repulsive force due to the magnetic gradient counteracts the attractive force of the currents, causing the islands to bounce. The evolution in this simple system depends on the complex interaction between the large-scale drive and the precise details of the ensuing reconnection.

In resistive magnetohydrodynamics (MHD), the occurrence of magnetic flux pileup [2] can render the reconnection rate insensitive to the plasma resistivity over a large range of Lundquist numbers (S). Here $S = 4\pi V_A L_{\rm sp}/\eta c^2$ where η is the resistivity, $L_{\rm sp}$ is the system size, and $V_A = B/\sqrt{4\pi m_i n}$ is the Alfvén velocity. Flux pileup weakens the dependence of the reconnection rate on S by allowing the upstream Alfvén speed (which limits the reconnection outflow speed) to increase as the resistivity drops. But several authors (e.g., [3]) have pointed out that this compensating increase in the upstream Alfvén speed must be limited by global momentum and energy conservation considerations: the upstream magnetic field must remain finite, and the upstream plasma pressure must remain positive. Thus, one expects pileup to saturate above some critical S, at which point the Sweet-Parker scaling reappears. More recent results suggest that the Sweet-Parker layer becomes unstable to secondary island generation at high S, allowing the coalescence to proceed at a higher rate than the Sweet-Parker scaling [4] but at the same time forcing the smallest scale current sheets to approach kinetic scales where MHD will clearly breakdown [5,6].

These issues have been examined in resistive Hall MHD [7]. For parameters where flux pileup occurs in resistive MHD, the Hall effect reduces the pileup and saturates it at a level which is independent of S. While this Hall pileup saturation phenomenon renders the reconnection rate insensitive to S in the low resistivity limit, the maximum rate scales as $\sqrt{d_i/\lambda}$ ([7,8]) where λ is the island size and d_i is the ion inertial length.

In contrast to the fluid results, previous studies of coalescence in the kinetic regime have found the islands to merge rapidly without any evidence for flux pileup [9]. However, these simulations were limited to small islands $\lambda \sim d_i$. In this Letter, we explore the interaction of large islands ($\geq 10 d_i$) and demonstrate, for the first time, the phenomenon of flux pileup saturation in the collisionless limit. However, there are significant differences with previous fluid results in all important aspects including the temporal evolution, the scaling of the reconnection rate, and amount of flux pileup with island size.

The simulations were performed with the fully kinetic particle-in-cell code VPIC [10] using the Fadeev [11] equilibrium which describes a chain of islands with vector potential $A_y(x, z) = -\lambda B_0 \ln[\cosh(z/\lambda) + \epsilon \cos(x/\lambda)]$. We added a 10% perturbation to this equilibrium, using the same functional form as in [5]. Here λ is the half-thickness of the current layer in the z direction, B_0 is the x component of the magnetic field upstream of the layer, and ϵ determines the initial island half-width

$L_i/\lambda = \cosh^{-1}(1+2\epsilon) \approx 2\epsilon^{1/2}(1-\epsilon/6+\ldots)$. For all simulations in this study, $\epsilon = 0.4$ so that $L_i \approx 1.2\lambda$. The density is given by $n(x) = n_0(1-\epsilon^2)/[\cosh(z/\lambda) + \epsilon\cos(x/\lambda)]^2 + n_b$ where n_0 is a reference density associated with the layer and n_b is an additional nondrifting uniform background with $n_b = 0.2n_0$. The temperatures are equal for both species $T_e = T_i = T_0$ including the background. Other parameters are $m_i/m_e = 25$, $\omega_{pe}/\Omega_{ce} = 2$, $\omega_{pe} = \sqrt{(4\pi n_0 e^2)/m_e}$ is the electron plasma frequency, Ω_{ce} is the electron gyrofrequency, and $v_{the}/c = (2T_0/m_e)^{1/2} = 0.35$. Lengths are normalized to the ion inertial scale $d_i = c/\omega_{pi}$ where $\omega_{pi} = \sqrt{(4\pi n_0 e^2)/m_i}$. The local ion inertial length based on the time evolving density is defined as d_i^*.

In comparing results from different runs, time is normalized to $t_A = L_x/V_A$, where V_A is based on n_0 and B_0 and $L_x = 4\pi\lambda$ is the system size in the x direction for the coalescence of two islands. Magnetic field is normalized to the initial peak value of the field along the line connecting the center of the two islands B', and $B_{\max}$ is the maximum pileup magnetic field using this normalization. We define the raw reconnection rate as $E_R \equiv (1/B'V_A')\partial\psi_r/\partial t$ where $\psi_r \equiv [\max A_y - \min A_y]_{z=0}$ is the reconnected flux and $V_A' \equiv B'/\sqrt{4\pi m_i n_0}$.

We conducted 6 runs for a range of islands from λ of $5d_i$ to $100d_i$ as summarized in Table I. The spatial resolution was higher than 1.4 times the Debye length in all the runs with the largest run consisting of $17\,920 \times 8960$ cells and an average of 250 particles per cell for each species. Time step is $\Delta t\Omega_{ce} = 0.12$. The boundary conditions are periodic in the x direction while the z boundaries are conducting for fields and reflecting for particles.

Figure 1(a) shows the intensity plot of B_y at $t = t_B$ for run $\lambda = 25d_i$. The thickness of the current sheet has dropped to below d_i at this point and the usual quadrupole pattern in B_y associated with reconnection is clearly evident. The stack plot of the total magnetic field $B_{\rm tot}$ in Fig. 1(b) illustrates the piling up of the magnetic field and a corresponding density depression. Also evident is the generation of obliquely propagating Alfvén waves upstream of the current sheet generated due to the sloshing back and forth of the islands as they merge. Consistent with their Alfvénic nature, there is only a weak density compression associated with these waves [Fig. 1(c)].

Comparative study of results of the 6 cases in Table I indicates that the details of the coalescence depend strongly on the initial island size. We have identified three distinct regimes of small ($\lambda \lesssim 10d_i$), medium ($\lambda \lesssim 50d_i$), and large ($\lambda \gtrsim 100d_i$) islands. A stack plot of $B_{\rm tot}$ as shown in Fig. 2 provides a quick summary of the time evolution of the system. The first phase of evolution is qualitatively similar in all three cases. The current sheet between the islands gets compressed and reaches its minimal thickness within $t \sim 1t_A$. Flux pileup also reaches its maximum value during this phase. The pileup is weak in the $\lambda = 5d_i$ case but is still evident. Beyond this point, there are important differences between the three cases. For $\lambda = 5d_i$, the current sheet remains thin, coalescence is rapid and the two islands fully merge before $t = 3t_A$. Coalescence is significantly slower for the other two cases, and for $\lambda = 100d_i$ the current sheet is seen to become dramatically thicker after the first phase, due to violent

TABLE I. Comparison of key parameters from each run. Listed are the island size λ, the time of the maximum pileup (t_B), time for peak reconnection rate t_R, the maximum pileup $B_{\max}$, the maximum reconnection rate normalized based on density and magnetic field values upstream of the ion diffusion region ($\tilde{E}_{R_{\max}}$), raw reconnection rate E_R averaged over $t = 2t_A$ ($\langle E_R\rangle$), and the separation distance of the two islands at the time of maximum magnetic field pileup ($L_{\rm sep}$) normalized to the initial island separation distance (L_0). L_0 is measured as the distance between the two initial 0 points.

λ/d_i	t_B/t_A	t_R/t_A	$B_{\max}$	$E_{R_{\max}}$	$\tilde{E}_{R_{\max}}$	$\langle E_R\rangle$	$L_{\rm sep}/L_0$
5	0.86	0.76	1.39	0.49	0.44	0.19	0.46
10	0.96	0.72	2.04	0.28	0.54	0.14	0.41
15	0.95	0.73	2.19	0.2	0.632	0.1	0.42
25	0.92	1.26	2.43	0.25	0.11	0.09	0.45
50	0.89	1.05	2.57	0.22	0.12	0.06	0.48
100	0.83	0.98	2.03	0.22	0.089	0.04	0.58

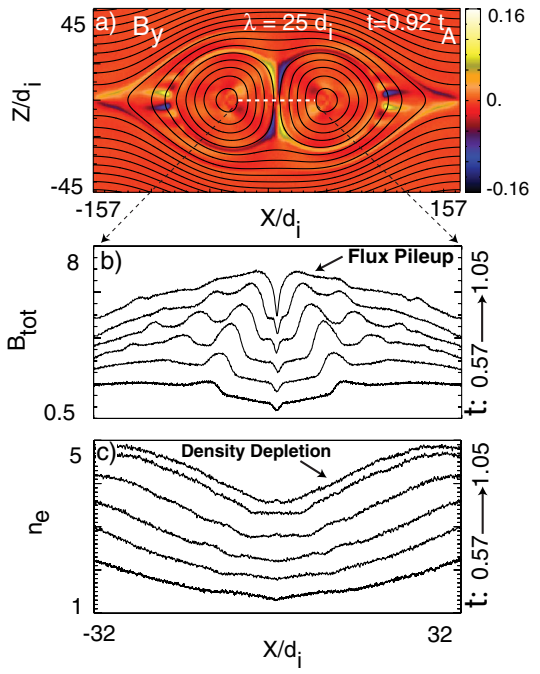

FIG. 1 (color online). Demonstration of magnetic flux pileup in the collisionless regime. (a) Intensity plot of B_y and formation of the quadrupole structure in the current sheet between the two islands for run $\lambda = 25d_i$. One-dimensional cuts of (a) total magnetic field and (b) electron density along the $Z = 0$ axis [dashed line Fig. 1(a)] stacked in time.

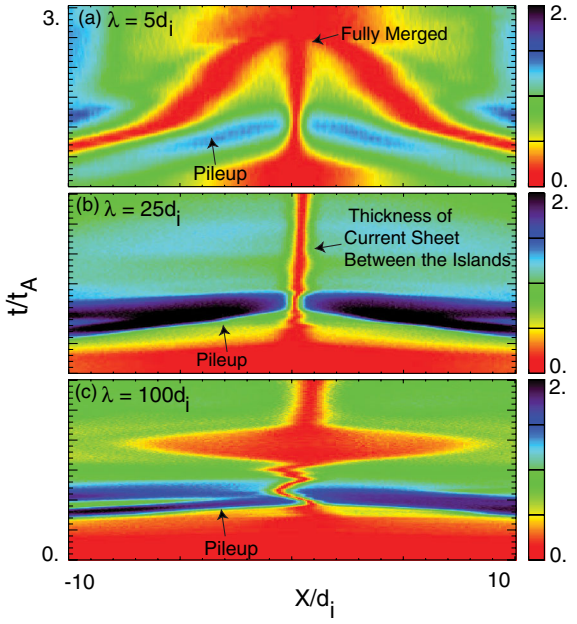

FIG. 2 (color online). Cuts of total magnetic field at $Z = 0$ stacked in time for the three runs $\lambda = 5$, 25, and $100d_i$.

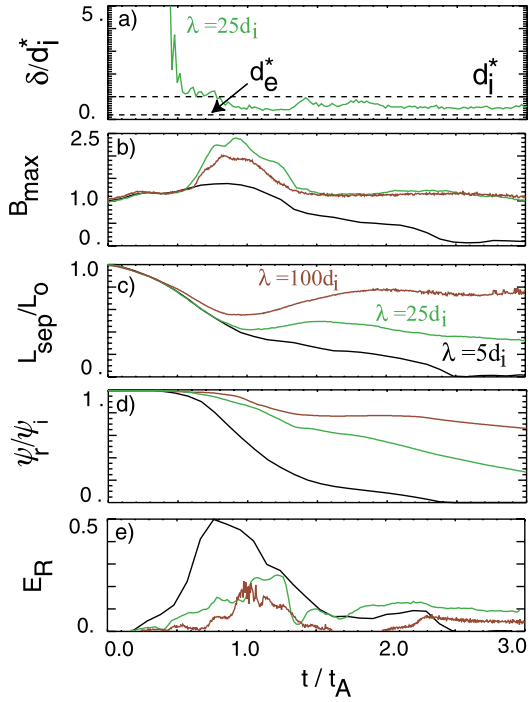

FIG. 3 (color online). Comparative time evolution of three runs representing the small, medium, and large island regimes. (a) Current sheet thickness normalized to the local ion inertial length versus time for $\lambda = 25d_i$. The two dashed lines correspond to the local ion d_i^* and electron d_e^* inertial lengths, respectively. Time variations of (b) maximum upstream magnetic field $B_{\max}$, (c) the separation of islands normalized to their initial separation distance, (d) reconnected flux normalized to the initial available flux, and (e) raw reconnection rate.

bouncing of the islands, before it settles down to a thickness greater than d_i.

Figure 3 provides more quantitative diagnostics for these three cases. While small islands exhibit at most a weak pileup $B_{\max}$, the medium and large island regimes are marked by a strong pileup of $B_{\max} \sim 2.5$. The peak pileup becomes nearly independent of island size in the medium and large island regimes (Table I). The island separation distance L_{sep} is shown in Fig. 3(c) as a function of time, and is normalized by the initial separation L_0. Unlike the $\lambda = 5d_i$ case, larger islands $\lambda = 25d_i$ and $100d_i$ show clear bouncing. The separation of islands is strongly correlated with the reconnected flux ψ_r normalized to the available flux ψ_i [Fig. 3(d)] as well as the reconnection rate [Fig. 3(e)]. This is because the onset of fast collisionless reconnection requires the current sheet to reach kinetic scales. As Fig. 3(a) indicates, the thickness of the current sheet normalized to the time evolving local d_i^* for $\lambda = 25d_i$ remains below the local ion inertial length after the first phase, thus enabling the islands to continue coalescing. This is in contrast to the $\lambda = 100d_i$ case (not shown) where the thickness stays above d_i^* after the first bounce. Note that after the first bounce for $\lambda = 100d_i$, there is little change in the separation of the islands and reconnection is essentially terminated.

One of the fundamental questions in reconnection physics is the efficiency in large systems and the amount of flux that is reconnected. To address this question, much focus has been placed on scaling of the peak reconnection rate with system size. Examination of the peak rate ($E_{R_{\max}}$) (Table I and Fig. 3) shows that aside from the initial drop of the rate from $\lambda = 5d_i$ to $\lambda = 10d_i$, the rate becomes nearly independent of system size. However, the peak rate only measures a transient response of the system and can only be related to the level of reconnected flux if the rate remains fixed in time. In a time dependent system, it is more appropriate to measure the amount of reconnected flux averaged over some macroscopic time scale which we take to be $t = 2t_A$. This choice ensures that the system has sufficient time to get past the initial transitory stage but other choices $t = 1$, 1.5, $3t_A$ give qualitatively similar results.

The ratio of ψ_r/ψ_i versus island size is shown in Fig. 4(a) and remarkably exhibits a $\sqrt{d_i/\lambda}$ dependence. We do not currently have an explanation for the observed form of this scaling. While this scaling implies that the fraction of reconnected flux decreases with island size, the total amount of reconnected flux may still be significant and is larger than that for smaller islands [Fig. 4(b)].

Despite some similarities to fluid results, there are significant differences in the details. Even in the presence of strong Hall electric fields, fluid theory predicts that magnetic pileup would (in the high S limit) scale as $E_{R_{\max}}\sqrt{\lambda/d_i}$. In the presaturation regime, $E_{R_{\max}}$ is independent of system size and the flux pileup $B_{\max}$ would increase

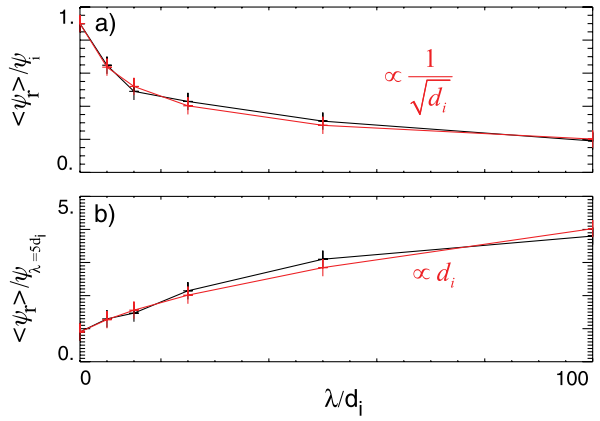

FIG. 4 (color online). Scaling with initial island size (λ) of reconnected flux averaged over $t = 2t_A$ normalized to (a) the initial available flux and (b) initial available flux of $\lambda = 5d_i$ case. The results exhibit $\sqrt{d_i/\lambda}$ and $\sqrt{\lambda/d_i}$ scalings, respectively.

with system size. As previously noted, the conservation laws impose an upper limit to the pileup, causing a saturation independent of island size. Thus the reconnection rate $E_{R_{\max}}$ must decrease as $\sqrt{d_i/\lambda}$ in the post-saturation regime. In contrast to these predictions [8,12], we find that both $E_{R_{\max}}$ and $B_{\max}$ are nearly independent of system size for the medium and large island limits (Table I) while the reconnection rate averaged over $t = 2t_A$, a quantity not measured in previous fluid studies, exhibits $\sqrt{d_i/\lambda}$ scaling. Another difference is in the electron and ion outflow speeds that are typically lower than the electron and ion Alfvén speeds, respectively. For example, for the $\lambda = 100d_i$ case, the peak electron (ion) outflow speed is 0.24 (0.46) times the electron (ion) Alfvén speed. This is clearly very different than the fluid models where the outflow speeds are Alfvénic [7]. These discrepancies point to the need as well as difficulties in developing appropriate fluid closures for collisionless plasmas.

The results obtained here may have profound implications for reconnection in planetary magnetospheres, solar wind, and solar corona. In the Earth's magnetosphere observations of plasma depletion layer (PDL) exhibit an increase in the magnetic field and a corresponding decrease in density [13]. It has been postulated that PDLs may be linked to flux pileup reconnection [14]. Our finding that flux pileup reconnection can occur in the collisionless regime provides support for this possibility. The result that merging is increasingly ineffective for larger islands imposes limitations on how large islands can grow through coalescence. Another implication of this work concerns the electron acceleration to 10–100 times v_{the} inferred in the interaction of flux ropes (magnetic clouds) in the solar wind [15]. Direct acceleration of electrons in the reconnection process requires low electron beta $\beta_e = 8\pi nT_e/B^2 \ll 1$ [16]. Magnetic clouds typically have $\beta_e \leq 0.3$ but to generate the required energetic electrons, β_e has to be $\sim$0.05. Flux pileup could provide a natural mechanism to lower β_e by $\sim$8 upstream of the current sheet between the islands, enabling enhanced electron acceleration in the process.

We emphasize that this is the first study of island coalescence as a function of island size in the kinetic regime and much work remains to establish the effects of guide field, β_e and other parameters on the details of the coalescence process. Three-dimensional effects also need to be explored. Our preliminary results suggest that the basic physics described here (e.g., bouncing, island size dependence, etc.) remains intact in other plasma parameter regimes. However, details can be different. For example, it appears that bouncing occurs for smaller islands in the presence of a finite guide field.

Authors acknowledge NSF Grants No. ATM0802380 and No. OCI 0904734, NASA Heliophysics Theory Program, and the LDRD program at Los Alamos. Simulations were performed on Kraken provided by the NSF at NICS and on Pleiades provided by NASA's HEC Program.

[1] D. Biskamp and K. Schindler, Phys. Plasmas **13**, 1013 (1971); J. M. Finn and P. Kaw, Phys. Fluids **20**, 2140 (1979); P. L. Pritchett and C. C. Wu, Phys. Fluids **22**, 2140 (1979); T. P. Intrator, X. Sun, and G. Lapenta *et al.*, Nature Phys. **5**, 521 (2009).
[2] E. N. Parker, Plasma Phys. **9**, 49 (2009); E. R. Priest and T. G. Forbes, J. Geophys. Res. **91**, 5579 (1986).
[3] Y. E. Litvinenko, Sol. Phys. **186**, 291 (1999).
[4] H. Karimabadi *et al.*, J. Geophys. Res. **109**, A09205 (2004); N. F. Loureiro, A. A. Schekochihin, and S. C. Cowley, Phys. Plasmas **14**, 100703 (2007); G. Lapenta, Phys. Rev. Lett. **100**, 235001 (2008); Yi-Min Huang and A. Bhattacharjee, Phys. Plasmas **17**, 062104 (2010).
[5] W. Daughton *et al.*, Phys. Rev. Lett. **103**, 065004 (2009).
[6] L. S. Shepherd and P. A. Cassak, Phys. Rev. Lett. **105**, 015004 (2010).
[7] J. C. Dorelli, Plasma Phys. **10**, 3309 (2003).
[8] D. A. Knoll and L. Chacón, Phys. Rev. Lett. **96**, 135001 (2006).
[9] P. L. Pritchett, Phys. Plasmas **14**, 052102 (2007).
[10] K. J. Bowers, B. J. Albright, and L. Yin *et al.*, Phys. Plasmas **15**, 055703 (2008).
[11] V. M. Fadeev, I. F. Kvartskhava, and N. N. Komarov, Nucl. Fusion **5**, 202 (1965).
[12] J. C. Dorelli and J. Birn, J. Geophys. Res. **108**, 1133 (2003).
[13] B. J. Anderson, T.-D. Phan, and S. A. Fuselier, J. Geophys. Res. **102**, 9531 (1997).
[14] J. C. Dorelli *et al.*, J. Geophys. Res., **109**, A12216 (2004).
[15] N. Gopalswamy, S. Yashiro, and M. L. Kaiser *et al.*, Astrophys. J. **548**, L91 (2001).
[16] J. Egedal *et al.*, Phys. Plasmas, **16**, 050701 (2009).